

# Effects of Annealing on Structural and Optical Characterization of Nanostructured ZnS Thin Films

Yasir Ismael Al-Rikabi

Department of Science, College of Basic Education, University of Diyala, Iraq.

Ban A. Bader

Department of Physics, College of Education, University of Al-Hamdaniya, Al-Hamdaniya, Nineveh, Iraq.

Mohammed Jawad Kadhim

Department of Radiology and Sonar, Al-Manara College for Medical Science, Iraq.

Nadir Fadhil Habubi

Department of Physics, College of Education, Mustansiriyah University, Iraq.

Sami Salman Chiad\*

Department of Physics, College of Education, Mustansiriyah University, Iraq.

## Abstract:

Nanostructured ZnS films were deposited via chemical spray pyrolysis (CSP) method. These films were deposited at annealing ( $T_a$ ) of (300, 400 and 500) °C. XRD analysis assures film polycrystallinity with predominant orientation along (200). The peak intensity was increased with increase of annealing. Microstrain and the dislocation density decreased with increase of annealing, indicating the enhancement of crystal quality. The optical transition was direct allowed to band gap energies between 3.19 and 3.06 eV depending on annealing. AFM results confirm that average particle size increase from (50 to 80) nm and average roughness decrease with increase of  $T_a$ .

**Keywords:** ZnS, spray pyrolysis, annealing, structural, Optical.

## 1-Introduction

ZnS is wide bandgap semiconductor, belongs to II–VI group. ZnS occur in two crystallographic shapes that possess a cubic zinc blend or hexagonal wurtzite structure [1]. The band gap of cubic lies between 3.54–3.6 eV, while for hexagonal was in the range of 3.74–3.87 eV [2]. ZnS films have many applications in optoelectronic device such as LED [3, 4], solar cells [5], gas sensors [6], antibacterial [7]. Various techniques were used to deposited ZnS such as sol-gel [8], Successive ionic layers adsorption and reaction [9], CVD [10], CSP [11-13], MBE [14], hydrothermal [15], RF Reactive Sputtering [16], wet chemistry processes [17]. Many researchers are working on the fabrication of ZnS films by CSP, because of it is simple, low cost and better control over the substrate. Besides the films have acceptable homogeneity. [40-60] This study was focused on the relationship between annealing temperature and surface morphology of nanostructured ZnS thin films by CSP.

## Experimental

ZnS films are grown via CSP method. A solution containing 0.1 M  $ZnCl_2$  and  $SC(NH_2)_2$  resolved in redistilled water to get ZnS. The nozzle was put at 29 cm over the base. flow rate 5ml/ min, spraying time was 8 s, waiting 2 min to restrain cooling, transporter gas was air keeping on  $10^5$  Pascal. Film thickness is measured by gravimetric method, their values were in the domain of  $350 \pm 35$  nm. Substrate temperature was utilized 300 °C. Transmittance is recorded via double beam spectrophotometer. High accuracy X-ray (Shimadzu, model: XRD-6000, Japan) is used to measure film structure, AFM was applied to find out surface topography.

## Result and Discussion

Fig.1 offers XRD styles of nanostructured ZnS. The film was revealed with high intensity peak oriented along (200) plane. This was compatible with the zinc blend structure according to (JCPDS card No.55-0566). Table 1 shows the average crystallite size ( $D$ ) is increasing with  $T_s$  increase from 31.27 to 36.49nm, resulting in grain growth, which agrees well with Haque et al. [17],  $D$  was calculated by using Scherrer's formula [18-21]:

$$D = \frac{0.94\lambda}{\beta \cos\theta} \quad (1)$$

Where  $\lambda = 1.54184\text{\AA}$ ,  $\theta$  is Bragg's angle and  $\beta$  FWHM. The dislocation density ( $\delta$ ), is calculated by [22-25]:

$$\delta = \frac{1}{D^2} \quad (2)$$

The microstrain ( $\epsilon$ ) was predestined using the equations [26-29]:

$$\epsilon = \frac{\beta \cos\theta}{4} \quad (3)$$

These structural parameters are represented in Table 1. Fig. 2 indicate the increment of  $D$  with the decrease of microstrain and dislocation density.

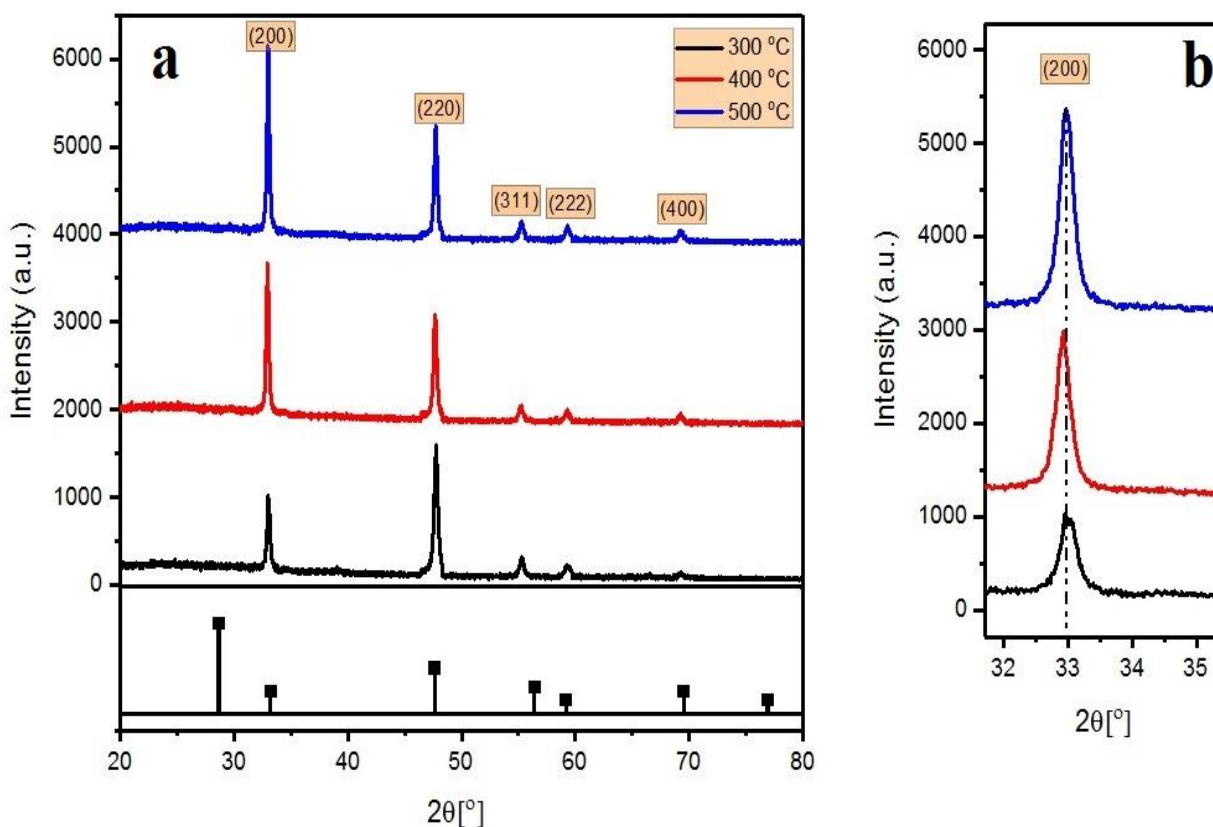


Figure 1. XRD styles of the growing films.

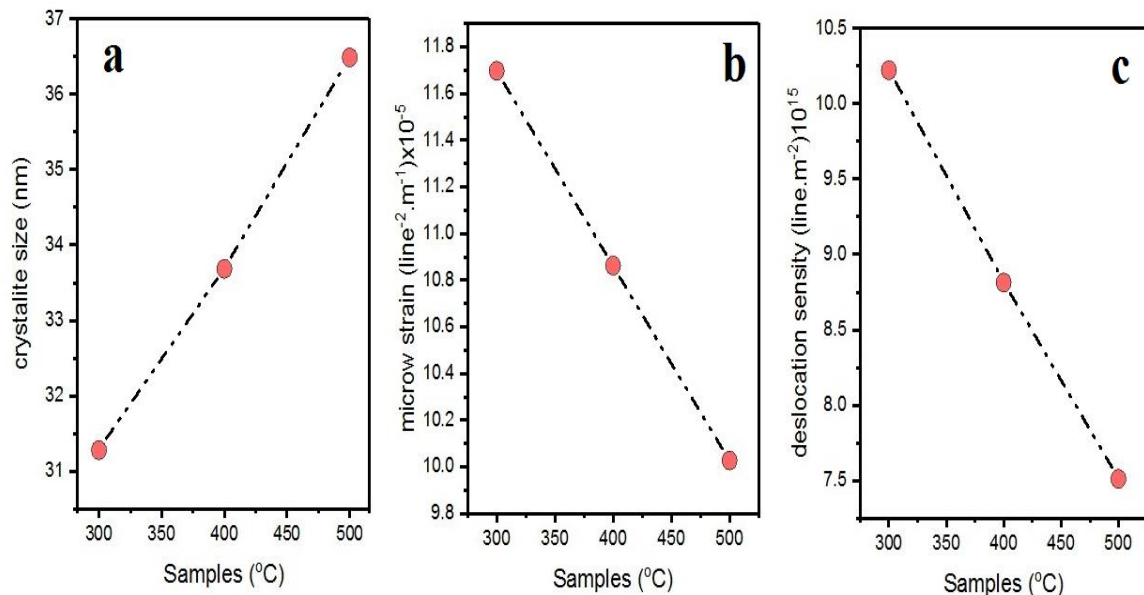


Figure 2. Structural parameter of growing films deposited at various Ta.

Table 1. S<sub>P</sub> of the intended films

Sample (°C)	(hkl) Plane	2theta (Deg.)	Lattice constant a (Å)	FWHM (Rad)	D (nm)	$\epsilon$ (line <sup>-2</sup> .m <sup>-1</sup> ) × 10 <sup>-3</sup>	Dislocation density( $\delta$ ) (line.m <sup>-2</sup> ) × 10 <sup>15</sup>
300	(200)	32.95	5.406	0.28	31.2776	11.69	10.22
400	(200)	32.95	5.406	0.26	33.6835	10.86	8.81
500	(200)	32.95	5.406	0.24	36.4905	10.02	7.51

Fig. (3, 4, 5) shows the AFM used to determine the distribution of the particle size and calculate the particle size of ZnS films grown at 300, 400 and 500 °C annealing. Fig. (3a, 3b, and 3c), show the 2 and 3dimensional AFM images of ZnS Films. uniform particles and densely packed with average particle size (50.16-80.97) nm and average roughness (6.19-1.49) nm was noticed and the RMS was in the zone of (7.22–1.72) nm. AFM result illustrates that average particle size increase and average roughness decrease with the increase of substrate temperature indicating that films improved in crystallinity and decrease in defects and these values proved the film nanocrystalline.

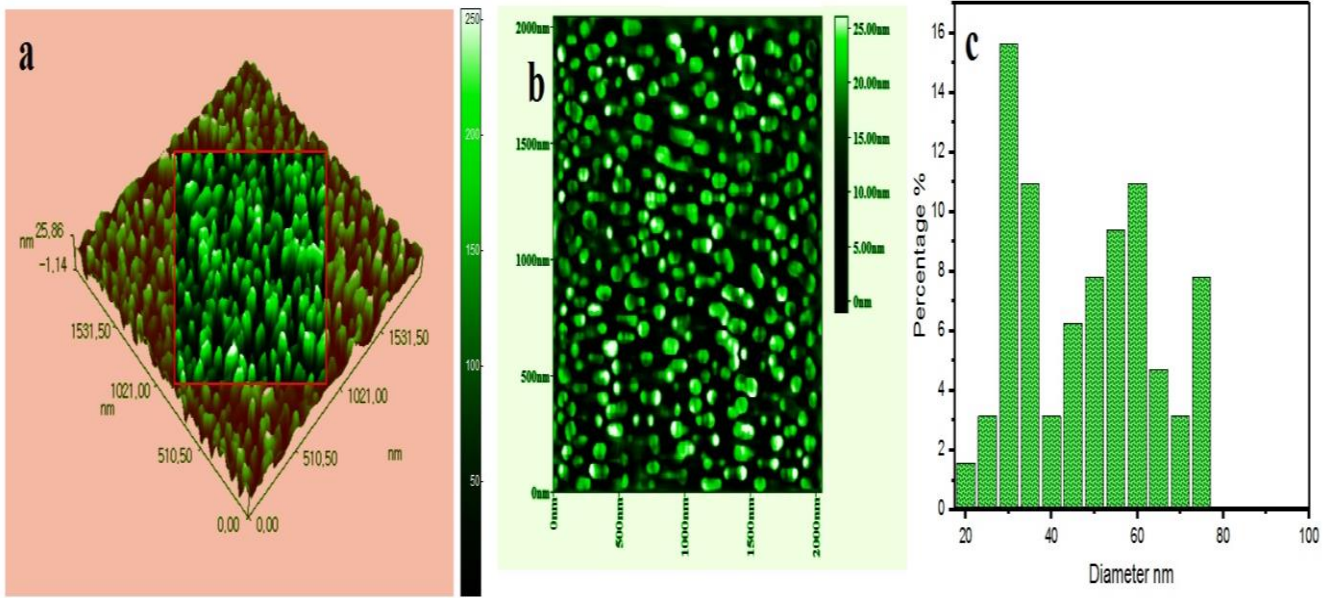


Figure 3. AFM Images of growing films at 300 °C.

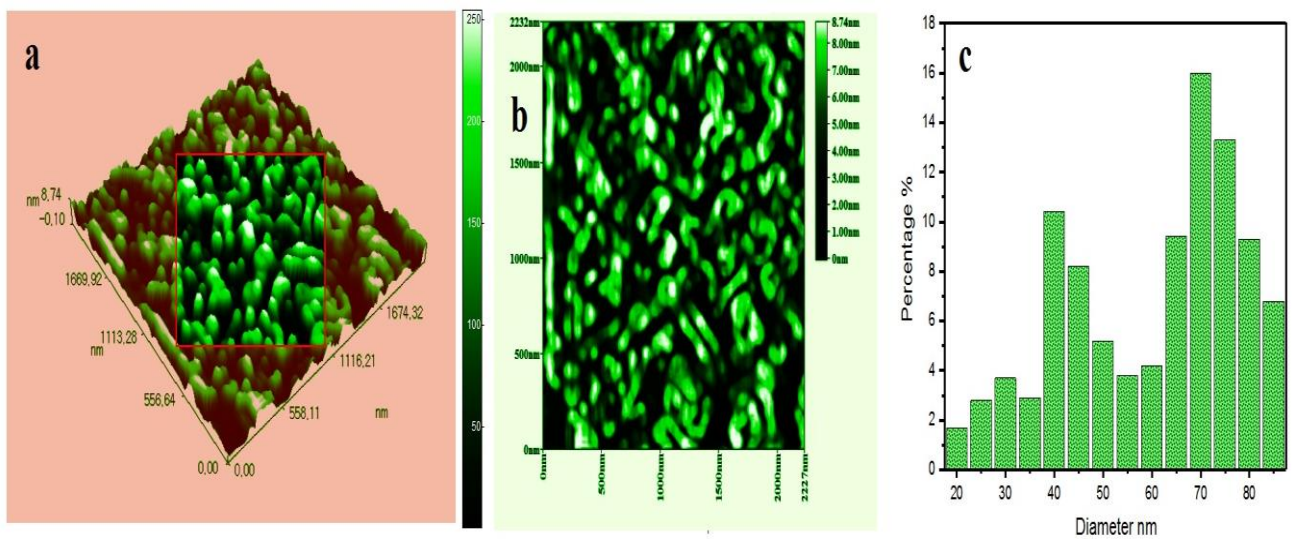


Figure 4. AFM Images of growing films at 400 °C.

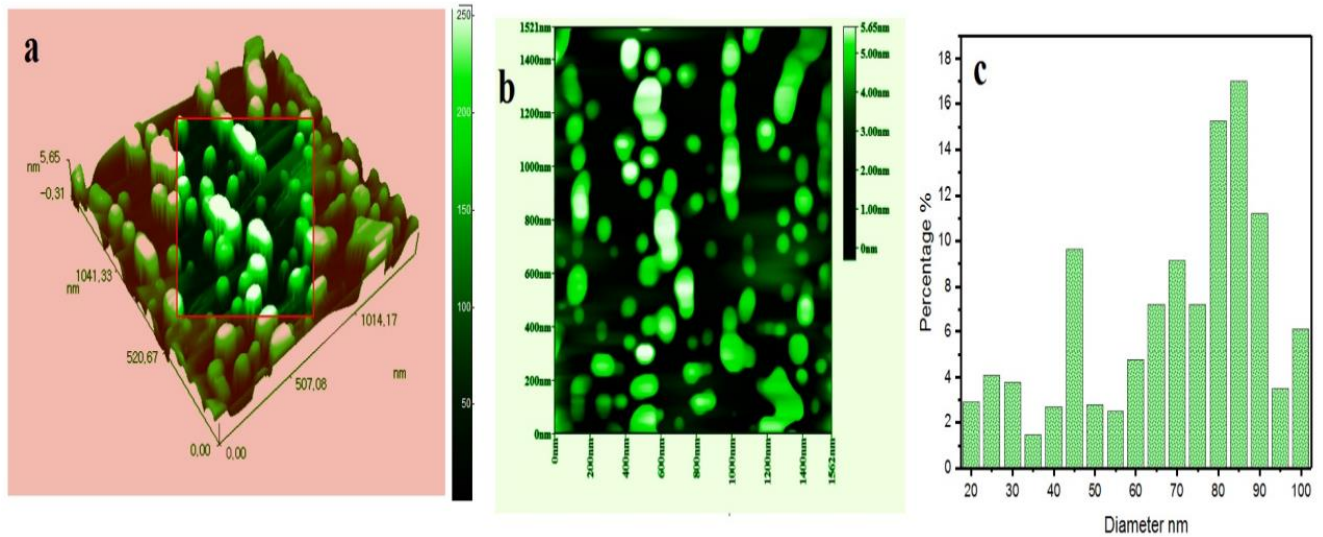


Figure 5. AFM Images of growing films at 500 °C.

Table2. Surface topography of ZnS films at various  $T_a$ .

Samples (°C)	Average particle size (nm)	Average roughness (nm)	RMS (nm)
300	50.16	6.19	7.22
400	60.12	2.02	2.37
500	80.97	1.49	1.72

Transmittance (T) spectra of ZnS films are displayed in Figure 6. Transmittance increases in the range of (55-80) % with increasing  $T_a$  up to 300°C (55-80) % from 500-900nm.

The absorption coefficient ( $\alpha$ ) was calculated using the equation [30-33]:

$$\alpha = \frac{1}{t} \ln \frac{1}{T} \quad \text{--- (4)}$$

Where t is the film thickness. Fig. 7 displays  $\alpha$  of samples at various  $T_a$ . The absorbance increased slightly with increasing the  $T_a$  of the deposition and the values of ( $\alpha > 10^4 \text{ cm}^{-1}$ ). The absorption coefficient is shifted toward lower wavelength of the grown films at low  $T_a$ . These results are fit well with references [34,35].

Tauc's relation was used to set band gap energy  $E_g$  [36-39], via a plot of  $(\alpha h\nu)^2$  as a function of  $h\nu$  (as shown in Figure 8).

$$(\alpha h\nu) = A(h\nu - E_g)^n \quad \text{--- (5)}$$

For direct transition  $n = \frac{1}{2}$ . Where A is a constant,  $\alpha$  is the absorption coefficient,  $h\nu$  is the energy of incident photon. It was noticed that  $E_g$  value decreases with increasing  $T_a$ ; 3.19 eV for 300°C compared to 3.06 eV for 500°C. This could be assigned to quantum size effect.

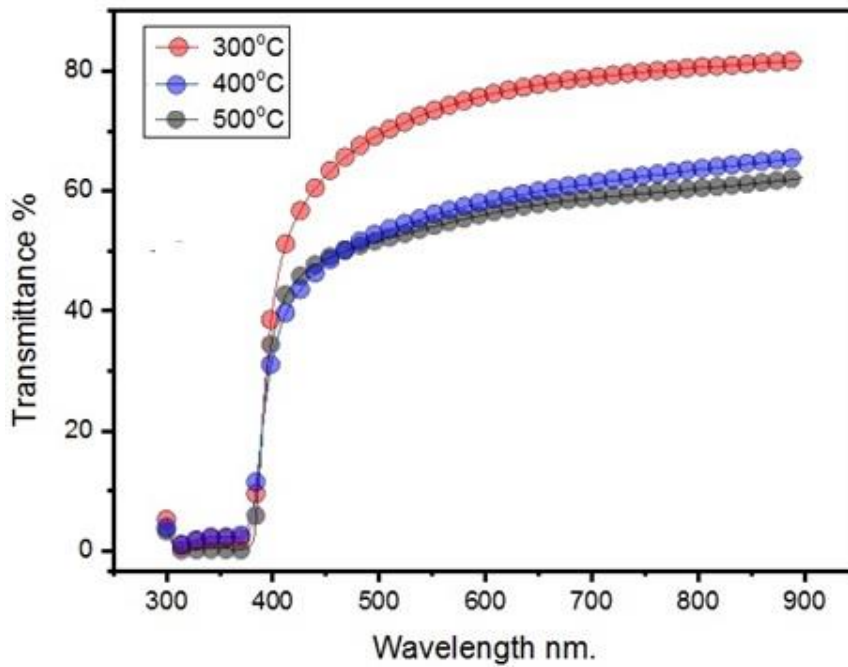


Figure 6. Transmittance of growing films at various  $T_a$ .

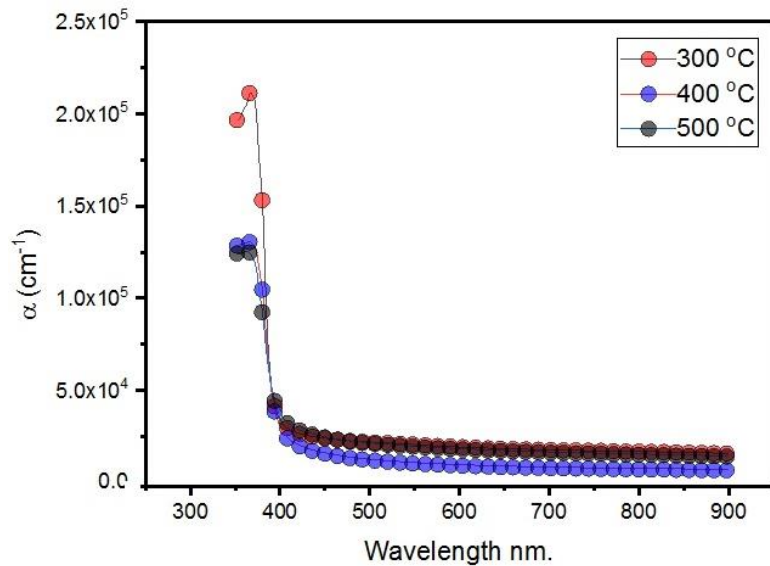


Figure 7. Absorption coefficient of growing films at various  $T_a$ .

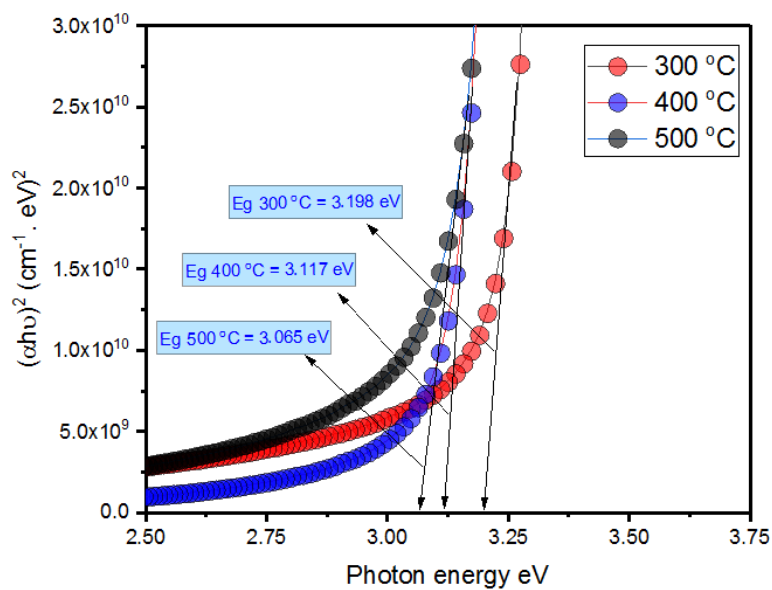


Figure 8. Energy gap of growing films at various  $T_s$ .

## Conclusions

ZnS thin films are grown by a CSP method onto glass substrate at various  $T_a$  of (300, 400 and 500) °C. The XRD analysis emphasizes the formation of polycrystalline ZnS with high peak intensity along (200) plane, which increases with the increase in  $T_a$ . Microstrain and dislocation density was decreased with an increase in  $T_a$ . Transmittance increases in the range of (55-80) % with increasing  $T_a$  the value of band gap energy  $E_g$  decrease with increasing  $T_a$ . The absorption coefficient is shifted toward lower wavelength for as-deposited at low substrate temperature. AFM result illustrates that average particle size increase (50-80) nm and average roughness decrease (6.19-1.49) nm with increase of substrate temperature indicating that improvement in film crystallinity.

## Acknowledgments

The authors thank Mustansiriyah University ([www.uomustansiriyah.edu.iq](http://www.uomustansiriyah.edu.iq)) for their support.

## References

[1] S. D. Scott and H. L. Barnes. Sphalerite–wurtzite equilibria and stoichiometry. *Geochimica et Cosmochimica Acta*, 36 (1972) 1275– 1295.

- [2] L. X. Shao, K. H. Chang and H. L. Hwang, inc sulfide thin films deposited by RF reactive sputtering for photovoltaic applications”, *Applied Surface Science*, 212–213 (2003)305–310. [3] R. H. Mauch, *Electroluminescence in thin films*, *Appl. Surf. Sci.*, 12 (1995) 589-597.
- [4] S. H. Deulkara, C. H. Bhosaela, M. Sharonb, *J. Phys. Chem. Solids* 65,1879(2004).
- [5] M. Leskela, *J. Alloys and Comp.*, 702 (1998) 275-278.
- [6] J. Vidol, O. de Melo, O. Vigil, N. Lopez, G. Contreras-Puent and O. Zelaya-Angel, *Thin Solid Films*, 118 (2002) 419 .
- [7] T. L. Chu, S. S. Chu, J. Brittrand, C. Ferekides and C. Q. Wu in: *Proceedings of the 22 nd IEEE Photovoltaic Specialists Conference, USA*,p.1136(1991).
- [8] K. Qiu, D. Qiu, L. Cai et al., “Preparation of ZnS thin films and ZnS/p-Si heterojunction solar cells,” *Materials Letters*, 198 (2017) 23–26.
- [9] W. Du, J. Yang, Y. Zhao, and C. Xiong, “Preparation of ZnS by magnetron sputtering and its buffer effect on the preferential orientation growth of ITO thin film,” *Micro & Nano Letters*, 13 (4) (2018) 506–508.
- [10] T. Hurma, Structural and optical properties of nanocrystal- line ZnS and ZnS:Al films, *Journal of Molecular Structure*, 1161 (2018) 279–284,.
- [11] T. Zscheckel, W. Wisniewski, A. Gebhardt, and C. Rüssel, “Recrystallization of CVD-ZnS during thermal treatment, *Optical Materials Express*, 4 (9) (2014).
- [12] Khadayeir, A.A., Jasim, R.I., Jumaah, S.H., Habubi, N.F., Chiad, S.S., Influence of Substrate Temperature on Physical Properties of Nanostructured ZnS Thin Films, *Journal of Physics: Conference Series*, 1664(1) (2020).
- [13] Ghazai, A.J., Abdulmunem, O.M., Qader, K.Y., Chiad, S.S., Habubi, N.F., Investigation of some physical properties of Mn doped ZnS nano thin films, *AIP Conference Proceedings* 2213 (1) (2020) 020101.
- [14] J. Bosco, F. Tajdar, and H. A. Atwater, “Molecular beam epi- taxy of n-type ZnS: a wide band gap emitter for heterojunction PV devices,” in 2012 38th IEEE Photovoltaic Specialists Confer ence, (2012) 2513–2517.
- [15] S. Yano, R. Schroeder, B. Ullrich, and H. Sakai, “Absorption and photocurrent properties of thin ZnS films formed by pulsed-laser deposition on quartz,” *Thin Solid Films*, 423 (2) (2003) 273–276.
- [16] R. Shahid, M. Gorlov, R. El-Sayed et al., Microwave assisted synthesis of Zns quantum dots using ionic liquids, *Materials Letters*, 89 (2012) 316–319.
- [17] V. Padmavathy, S. Sankar, and V. Ponnuswamy, Influence of thiourea on the synthesis and characterization of chemi- cally deposited nano structured zinc sulphide thin films, *Journal of Materials Science: Materials in Electronics*, 1 29 (9) (2018)7739–7749.
- [18] Abdulmunem, O.M., Jabbar, A.M., Muhammad, S.K., Dawood, M.O., Chiad, S.S., Habubi, N.F., Investigation of Co-doped Cu2O thin films on the structural, optical and morphology by SPT, *Journal of Physics: Conference Series*, 1660(1) (2020 ) 012055..
- [19] Hassan, E.S., Mubarak, T.H., Chiad, S.S., Habubi, N.F., Khadayeir, A.A., Dawood, M.O., Al-Baidhany, I.A., Physical Properties of indium doped Cadmium sulfide thin films prepared by (SPT), *Journal of Physics: Conference Series* 1294(2) 2019, 022008.
- [20] Hassan, E.S., Elttayef, A.K., Mostafa, S.H., Salim, M.H., Chiad, S.S., Silver oxides nanoparticle in gas sensors applications, *Journal of Materials Science: Materials in Electronics*, 30(17) (2019) 15943-15951.
- [21] Beevi M. M., Anusuya M., Saravanan V., *International Journal of Chemical Engineering and Applications*, 1 (2010)151-154.
- [22] Ali, R.S., Sharba, K.S., Jabbar, A.M., Chiad, S.S., Abass, K.H., Habubi, N.F., Characterization of ZnO thin film/p-Si fabricated by vacuum evaporation method for solar cell applications, 2020, *NeuroQuantology* 18(1) (2020) 26-31.
- [23] M. O. Dawood, S.S. Chiad, A. J. Ghazai, N. F. Habubi and O. M. Abdulmunem, Effect of Li doping on structure and optical properties of NiO nano thin-films by SPT, *AIP Conference Proceedings, USA*, 2213 (1) 1 (2020) 020102.
- [24] Mane RS and Lochande CD, Chemical deposition method for metal chalcogenide thin films, *Mater. Chem. Phys.*, 65 (2000) 1-31.
- [25] N. N. Jandow, N. F. Habubi, S. S. chiad, I. A. Al-Baidhany and M. A. Qaeed, Annealing Effects on Band Tail Width, Urbach Energy and Optical Parameters of Fe<sub>2</sub>O<sub>3</sub>:Ni Thin Films Prepared by Chemical Spray Pyrolysis Technique, *International Journal of Nanoelectronics and Materials, Malaysia*, 12 1 (2019) (1-10).
- [26] Ahmed, N.Y., Bader, B.A., Slewa, M.Y., Habubi, N.F., Chiad, S.S., Effect of boron on structural, optical characterization of nanostructured fe2o3 thin films, *NeuroQuantology*, 18(6) (2020) 55-60.
- [27] Chiad, S. S. and Mubarak, T. H.,The Effect of Ti on Physical Properties of Fe<sub>2</sub>O<sub>3</sub> Thin Films for Gas Sensor Applications, 2020, *International Journal of Nanoelectronics and Materials*, 13(2) (2020) 221-232.
- [28] Hadi, E.H., Sabur, D.A., Chiad, S.S., Habubi, N.F., Abass, K.H., Physical properties of nanostructured li-doped zro2 thin films, *Journal of Green Engineering*, 10(10) (2020) 8390-8400.
- [29] Hsu CT, Epitaxial growth of II–VI compound semiconductors by atomic layer epitaxy, *Thin Solid Films*, 335(1998) 284-291.
- [30] Muhammad, S. K., Hassan, E.S., Qader, K.Y., Abass, K.H., Chiad, S. S., Habubi, N. F., Effect of vanadium on structure and morphology of SnO<sub>2</sub> thin films, *Nano Biomedicine and Engineering*, 12 (1) (2020) 67-74.
- [31] Sakhil, M.D., Shaban, Z.M., Sharba, K.S., Habub, N.F., Abass, K.H., Chiad, S.S., Alkelaby, A.S., Influence mgo dopant on structural and optical properties of nanostructured cuo thin films, *NeuroQuantology*, 18 (5) (2020) 56-61.
- [32] Khadayeir, A. A., Hassan, E. S., Mubarak, T. H., Chiad, S.S., Habubi, N. F., Dawood, M.O., Al-Baidhany, I. A., The effect of substrate temperature on the physical properties of copper oxide films, *Journal of Physics: Conference Series*, 1294 (2) (2019) 022009.

- [33] Ahmed, F.S., Ahmed, N.Y., Ali, R.S., Habubi, N.F., Abass, K.H. and Chiad, S.S. Effects of Substrate Type on Some Optical and Dispersion Properties of Sprayed CdO Thin Films, *NeuroQuantology*, 18 (3) (2020) 56-65.
- [34] Haque, F., Rahman, K.S., Islam, M.A., Rasid, M.J., Alam, M.M., Alothman, Z.A., Soplan, K., Amin, N.: Growth optimization of ZnS thin films by R F Magnetron sputtering as prospective buffer layer in thin film solar cell. *Chalcogenide Lett.*, 11 (2014)189–197.
- [35] M. Nada Saeed, Structural and optical properties of ZnS thin films prepared by spray pyrolysis technique, *J. Al-Nahrain Univ.*, .14 (2011) 86–92.
- [36] Ban A. Bader, Shawki Khalaph Muhammad, Ali Mohammed Jabbar, Khalid Haneen Abass, Sami Salman Chiad and Nadir Fadhil Habubi, Synthesis and Characterization of Indium-doped CdO Nanostructured Thin Films: a Study on Optical, orphological, and Structural Properties, *J. Nanostruct* 10(4) (2020) 744-750.
- [37] Reem Sami Ali, Noor Al-Huda Al-Aaraji, Esraa H. Hadi, Khalid Haneen Abass, Nadir Fadhil habubi, Sami Salman Chiad, Effect of Lithium on Structural and Optical Properties of Nanostructured CuS Thin, *J. Nanostruct*, 10 (4) (2020) 810-816.
- [38] Ahmed, N.Y., Bader, B.A., Slewa, M.Y., Habubi, N.F., Chiad, S.S., Effect of boron on structural, optical characterization of nanostructured fe2o3 thin films, *NeuroQuantology*, 18(6) (2020) 55-60.
- [39] Chiad, S.S., Alkelaby, A.S., Sharba, K.S., Optical Conduct of Nanostructure Co3O4 rich Highly Doping Co3O4: Zn alloys, *Journal of Global Pharma Technology*, 11(7) (2020) 662-665.
- [40] JALIL, A. T., DILFY, S. H., KAREVSKIY, A., & NAJAH, N. (2020). Viral Hepatitis in Dhi-Qar Province: Demographics and Hematological Characteristics of Patients. *International Journal of Pharmaceutical Research*, 12(1). <https://doi.org/10.31838/ijpr/2020.12.01.326>
- [41] Dilfy, S. H., Hanawi, M. J., Al-bideri, A. W., & Jalil, A. T. (2020). Determination of Chemical Composition of Cultivated Mushrooms in Iraq with Spectrophotometrically and High Performance Liquid Chromatographic. *Journal of Green Engineering*, 10, 6200-6216.
- [42] Jalil, A. T., Al-Khafaji, A. H. D., Karevskiy, A., Dilfy, S. H., & Hanan, Z. K. (2021). Polymerase chain reaction technique for molecular detection of HPV16 infections among women with cervical cancer in Dhi-Qar Province. *Materials Today: Proceedings*. <https://doi.org/10.1016/j.matpr.2021.05.211>
- [43] Jalil, A. T., Kadhum, W. R., Khan, M. U. F., Karevskiy, A., Hanan, Z. K., Suksatan, W., ... & Abdullah, M. M. (2021). Cancer stages and demographical study of HPV16 in gene L2 isolated from cervical cancer in Dhi-Qar province, Iraq. *Applied Nanoscience*, 1-7. <https://doi.org/10.1007/s13204-021-01947-9>
- [44] Widjaja, G., Jalil, A. T., Rahman, H. S., Abdelbasset, W. K., Bokov, D. O., Suksatan, W., ... & Ahmadi, M. (2021). Humoral Immune mechanisms involved in protective and pathological immunity during COVID-19. *Human Immunology*. <https://doi.org/10.1016/j.humimm.2021.06.011>
- [45] Moghadasi, S., Elveny, M., Rahman, H. S., Suksatan, W., Jalil, A. T., Abdelbasset, W. K., ... & Jarahian, M. (2021). A paradigm shift in cell-free approach: the emerging role of MSCs-derived exosomes in regenerative medicine. *Journal of Translational Medicine*, 19(1), 1-21. <https://doi.org/10.1186/s12967-021-02980-6>
- [46] Hanan, Z. K., Saleh, M. B., Mezal, E. H., & Jalil, A. T. (2021). Detection of human genetic variation in VAC14 gene by ARMA-PCR technique and relation with typhoid fever infection in patients with gallbladder diseases in Thi-Qar province/Iraq. *Materials Today: Proceedings*. <https://doi.org/10.1016/j.matpr.2021.05.236>
- [47] Saleh, M. M., Jalil, A. T., Abdulkereem, R. A., & Suleiman, A. A. Evaluation of Immunoglobulins, CD4/CD8 T Lymphocyte Ratio and Interleukin-6 in COVID-19 Patients. *TURKISH JOURNAL of IMMUNOLOGY*, 8(3), 129-134. <https://doi.org/10.25002/tji.2020.1347>
- [48] Turki Jalil, A., Hussain Dilfy, S., Oudah Meza, S., Aravindhan, S., M Kadhim, M., & M Aljeboree, A. (2021). CuO/ZrO2 nanocomposites: facile synthesis, characterization and photocatalytic degradation of tetracycline antibiotic. *Journal of Nanostructures*.
- [49] Sarjito, Elveny, M., Jalil, A., Davarpanah, A., Alfakeer, M., Awadh Bahajjaj, A. & Ouladsmane, M. (2021). CFD-based simulation to reduce greenhouse gas emissions from industrial plants. *International Journal of Chemical Reactor Engineering*, (), 20210063. <https://doi.org/10.1515/ijcre-2021-0063>
- [50] Marofi, F., Rahman, H. S., Al-Obaidi, Z. M. J., Jalil, A. T., Abdelbasset, W. K., Suksatan, W., ... & Jarahian, M. (2021). Novel CAR T therapy is a ray of hope in the treatment of seriously ill AML patients. *Stem Cell Research & Therapy*, 12(1), 1-23. <https://doi.org/10.1186/s13287-021-02420-8>
- [51] Jalil, A. T., Shanshool, M. T., Dilfy, S. H., Saleh, M. M., & Suleiman, A. A. (2021). HEMATOLOGICAL AND SEROLOGICAL PARAMETERS FOR DETECTION OF COVID-19. *Journal of Microbiology, Biotechnology and Food Sciences*, e4229. <https://doi.org/10.15414/jmbfs.4229>
- [52] Vakili-Samiani, S., Jalil, A. T., Abdelbasset, W. K., Yumashev, A. V., Karpishev, V., Jalali, P., ... & Jadidi-Niaragh, F. (2021). Targeting Wee1 kinase as a therapeutic approach in Hematological Malignancies. *DNA repair*, 103203. <https://doi.org/10.1016/j.dnarep.2021.103203>
- [53] NGAFWAN, N., RASYID, H., ABOOD, E. S., ABDELBASSET, W. K., AL-SHAWI, S. G., BOKOV, D., & JALIL, A. T. (2021). Study on novel fluorescent carbon nanomaterials in food analysis. *Food Science and Technology*. <https://doi.org/10.1590/fst.37821>
- [54] Marofi, F., Abdul-Rasheed, O. F., Rahman, H. S., Budi, H. S., Jalil, A. T., Yumashev, A. V., ... & Jarahian, M. (2021). CAR-NK cell in cancer immunotherapy; A promising frontier. *Cancer Science*, 112(9), 3427. <https://doi.org/10.1111/cas.14993>



- [55] Abosooda, M., Wajdy, J. M., Hussein, E. A., Jalil, A. T., Kadhim, M. M., Abdullah, M. M., ... & Almashhadani, H. A. (2021). Role of vitamin C in the protection of the gum and implants in the human body: theoretical and experimental studies. *International Journal of Corrosion and Scale Inhibition*, 10(3), 1213-1229. <https://dx.doi.org/10.17675/2305-6894-2021-10-3-22>
- [56] Jumintono, J., Alkubaisy, S., Yáñez Silva, D., Singh, K., Turki Jalil, A., Mutia Syarifah, S., ... & Derkho, M. (2021). Effect of Cystamine on Sperm and Antioxidant Parameters of Ram Semen Stored at 4° C for 50 Hours. *Archives of Razi Institute*, 76(4), 923-931. <https://dx.doi.org/10.22092/ari.2021.355901.1735>
- [57] Roomi, A. B., Widjaja, G., Savitri, D., Turki Jalil, A., Fakri Mustafa, Y., Thangavelu, L., ... & Aravindhan, S. (2021). SnO<sub>2</sub>: Au/Carbon Quantum Dots Nanocomposites: Synthesis, Characterization, and Antibacterial Activity. *Journal of Nanostructures*.
- [58] Raya, I., Chupradit, S., Kadhim, M. M., Mahmoud, M. Z., Jalil, A. T., Surendar, A., ... & Bochvar, A. N. (2021). Role of Compositional Changes on Thermal, Magnetic and Mechanical Properties of Fe-PC-Based Amorphous Alloys. *Chinese Physics B*. <https://doi.org/10.1088/1674-1056/ac3655>
- [59] Chupradit, S., Jalil, A. T., Enina, Y., Neganov, D. A., Alhassan, M. S., Aravindhan, S., & Davarpanah, A. (2021). Use of Organic and Copper-Based Nanoparticles on the Turbulator Installment in a Shell Tube Heat Exchanger: A CFD-Based Simulation Approach by Using Nanofluids. *Journal of Nanomaterials*. <https://doi.org/10.1155/2021/3250058>
- [60] Raya, I., Chupradit, S., Mustafa, Y., H. Oudaha, K., M. Kadhim, M., Turki Jalil, A., J. Kadhim, A., Mahmudiono, T., Thangavelu, L. (2021). Carboxymethyl Chitosan Nano-Fibers for Controlled Releasing 5-Fluorouracil Anticancer Drug. *Journal of Nanostructures*,